2010

Stabilizing vehicle lateral dynamics with considerations of parameter uncertainties and control saturation through robust yaw control

Haiping Du
University of Wollongong, hdu@uow.edu.au

Nong Zhang
University of Technology, Sydney

Guangming Dong
Shanghai Jiaotong University

Stabilizing vehicle lateral dynamics with considerations of parameter uncertainties and control saturation through robust yaw control

Abstract

This paper presents a robust yaw-moment controller design for improving vehicle handling and stability with considerations of parameter uncertainties and control saturation. The parameter uncertainties dealt with are the changes of vehicle mass and moment of inertia about the yaw axis and the variations of cornering stiffnesses. The control saturation considered is due to the physical limitations of actuators and tires. Both polytopic and norm-bounded approaches are used to describe parameter uncertainties, and a norm-bounded approach is applied to handle the saturation nonlinearity. The conditions for designing such a controller are derived as linear matrix inequalities (LMIs). A nonlinear vehicle model is utilized to validate the effectiveness of the proposed approach. The simulation results show that the designed controller can improve vehicle handling and stability, regardless of the changes in vehicle mass and moment of inertia and the variations of road surfaces and saturation limitations.

Disciplines

Physical Sciences and Mathematics

Publication Details

H. Du, N. Zhang & G. Dong, "Stabilizing vehicle lateral dynamics with considerations of parameter uncertainties and control saturation through robust yaw control," IEEE Transactions on Vehicular Technology, vol. 59, (5) pp. 2593-2597, 2010.

Stabilizing Vehicle Lateral Dynamics With Considerations of Parameter Uncertainties and Control Saturation Through Robust Yaw Control

Haiping Du, Nong Zhang, and Guangming Dong

***Abstract*—This paper presents a robust yaw-moment controller design for improving vehicle handling and stability with considerations of parameter uncertainties and control saturation. The parameter uncertainties dealt with are the changes of vehicle mass and moment of inertia about the yaw axis and the variations of cornering stiffnesses. The control saturation considered is due to the physical limitations of actuators and tires. Both polytopic and norm-bounded approaches are used to describe parameter uncertainties, and a norm-bounded approach is applied to handle the saturation nonlinearity. The conditions for designing such a controller are derived as linear matrix inequalities (LMIs). A nonlinear vehicle model is utilized to validate the effectiveness of the proposed approach. The simulation results show that the designed controller can improve vehicle handling and stability, regardless of the changes in vehicle mass and moment of inertia and the variations of road surfaces and saturation limitations.**

***Index Terms*—Control saturation, parameter uncertainty, vehicle lateral dynamics, yaw moment control.**

I. Introduction

The control of ground-vehicle lateral dynamics to improve driver satisfaction and safety has become increasingly important. Combining electronic control systems with the existing hardware to maximize the system performance is increasingly regarded as a good way to do it. Strategies like vehicle dynamics control [1], [2], antilock braking systems [3], [4], active steering control [5], [6], direct yaw-moment control, etc., have been developed to allow the driver to keep control of the vehicle when the vehicle is at the physical limit of adhesion between the tires and the road. In particular, the yaw-moment control is proved to be one of the most promising means of chassis control, which could considerably enhance vehicle handling and active safety during severe driving maneuvers [7]. Various control methodologies, such as optimal control [8], fuzzy logic control [9], internal model control [10], flatness-based control [11], etc., have been proposed in the literature, and a recent review on vehicle chassis control schemes can be found in [12].

Vehicle load is one parameter that is easily varied due to the change of the number of passengers or the payload. Vehicle-load variation will accordingly change the vehicle mass, the moment of inertia, and the center of gravity (CG) location, which directly affect vehicle lateral dynamics and vehicle stability. Although the vehicle mass uncertainty could be dealt with by a μ-synthesis robust control approach [13], a high-order controller design made its implementation complicated. Other parameter uncertainties that affect vehicle lateral dynamics may come from tire–road conditions. Since the yaw-moment control obviously relies on the tire lateral force and the tire force strongly depends on tire vertical load, which is very sensitive to vehicle motion and environmental conditions, the tire cornering stiffness inevitably obtains uncertainties that need to be coped with. On the other hand, due to the physical limitations of actuators and tires, not every required yaw moment can ideally be generated. As a consequence, the control saturation aspect should be considered in the controller design process to make the implementation of controller more practical. In spite of their significance, it is noticed that not much effort has been made to consider vehicle load variation, tire cornering stiffness uncertainties, and control saturation problems in one research, which motivates our current study.

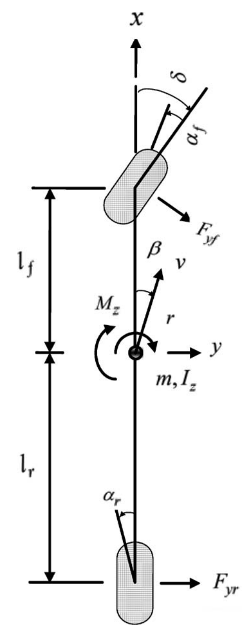

Fig. 1. Two degree-of-freedom model of vehicle dynamics.

In this paper, a robust yaw-moment controller is designed for a two-degree-of-freedom (2DOF) vehicle lateral dynamics model with considerations of vehicle load variation, cornering stiffness uncertainty, and control saturation. The control objective is to stabilize the closed-loop system with optimal performance on sideslip angle and yaw rate in the presence of parameter uncertainties and control saturation. The conditions for designing such a controller are derived as linear matrix inequalities (LMIs). Numerical simulations performed on a nonlinear vehicle model are used to validate the control performance of the designed controller.

The notation used throughout this paper is standard. For a real symmetric matrix W, the notation of $W > 0$ $(W < 0)$ is used to denote its positive (negative) definiteness. I is used to denote the identity matrix of appropriate dimensions. To simplify the notation, $*$ is used to represent a block matrix that is readily inferred by symmetry.

II. Description of Uncertain Vehicle Dynamics Model

In this paper, a bicycle model of vehicle dynamics, as shown in Fig. 1, is used for controller design. The vehicle has mass m and moment of inertia I_z about the yaw axis through its CG. The front

Manuscript received December 17, 2008; revised July 1, 2009 and January 13, 2010; accepted February 22, 2010. Date of publication March 15, 2010; date of current version June 16, 2010. The review of this paper was coordinated by Dr. S. Anwar.

H. Du is with the School of Electrical, Computer, and Telecommunications Engineering, University of Wollongong, Wollongong, NSW 2522, Australia (e-mail: hdu@uow.edu.au).

N. Zhang is with the Faculty of Engineering, University of Technology, Sydney, Sydney, NSW 2007, Australia.

G. Dong is with the State Key Laboratory of Vibration, Shock, and Noise, Shanghai Jiao Tong University, Shanghai 200240, China.

Color versions of one or more of the figures in this paper are available online at http://ieeexplore.ieee.org.

Digital Object Identifier 10.1109/TVT.2010.2045520

and rear axles are located at distances l_f and l_r, respectively, from the vehicle CG. The front and rear lateral tire forces F_{yf} and F_{yr} depend on slip angles α_f and α_r, respectively, and the steering angle δ changes the heading of the front tires.

The vehicle's handling dynamics in the yaw plane can be represented with states of sideslip angle β and yaw rate r as

$$\begin{aligned} mv\dot{\beta}(t) &= F_{yf}(t) + F_{yr}(t) - mvr(t) \\ I_z\dot{r}(t) &= l_f F_{yf}(t) - l_r F_{yr}(t) + M_z(t) \end{aligned} \tag{1}$$

where $M_z(t)$ is the external yaw moment, and v is the vehicle velocity that is assumed to be a constant in the study.

With low lateral acceleration, the tires operate in the linear region, and the lateral forces at the front and rear can be related to slip angles by the cornering stiffnesses of the front and rear tires as

$$\begin{aligned} F_{yf}(t) &= C_{\alpha f}\alpha_f(t) \\ F_{yr}(t) &= C_{\alpha r}\alpha_r(t) \end{aligned} \tag{2}$$

where $C_{\alpha f}$ and $C_{\alpha r}$ are the cornering stiffnesses for the front and rear tires, respectively. The front and rear slip angles are defined as

$$\begin{aligned} \alpha_f(t) &= \delta(t) - \frac{l_f r(t)}{v} - \beta(t) \\ \alpha_r(t) &= \frac{l_r r(t)}{v} - \beta(t). \end{aligned} \tag{3}$$

Substituting (2) and (3) into (1), equation (1) is expressed in state-space form as

$$\dot{x}(t) = Ax(t) + B_1 w(t) + B_2 u(t) \tag{4}$$

where

$$\begin{aligned} x(t) &= [\beta(t), \quad r(t)]^T \\ w(t) &= \delta(t), \quad u(t) = M_z(t) \\ A &= \begin{bmatrix} -\frac{C_{\alpha f}+C_{\alpha r}}{mv} & -1 - \frac{l_f C_{\alpha f} - l_r C_{\alpha r}}{mv^2} \\ -\frac{l_f C_{\alpha f} - l_r C_{\alpha r}}{I_z} & -\frac{l_f^2 C_{\alpha f} + l_r^2 C_{\alpha r}}{I_z v} \end{bmatrix} \\ B_1 &= \begin{bmatrix} \frac{C_{\alpha f}}{mv} \\ \frac{l_f C_{\alpha f}}{I_z} \end{bmatrix}, \quad B_2 = \begin{bmatrix} 0 \\ \frac{1}{I_z} \end{bmatrix}. \end{aligned}$$

As the varying vehicle mass m is actually bounded by its minimum value $m_{\min}$ and its maximum value $m_{\max}$ in a real operation, it is not difficult to represent the uncertain vehicle mass by

$$1/m = M_1(\xi_1) m_{s\max} + M_2(\xi_1) m_{s\min}$$

where $\xi_1 = 1/m$, $m_{s\max} = 1/m_{\min}$, $m_{s\min} = 1/m_{\max}$, and $M_1(\xi_1)$ and $M_2(\xi_1)$ are defined as

$$\begin{aligned} M_1(\xi_1) &= \frac{1/m - m_{s\min}}{m_{s\max} - m_{s\min}} \\ M_2(\xi_1) &= \frac{m_{s\max} - 1/m}{m_{s\max} - m_{s\min}}. \end{aligned} \tag{5}$$

Similarly, the uncertain moment of inertia I_z is bounded by its minimum value $I_{\min}$ and its maximum value $I_{\max}$ so that it can be represented by

$$1/I_z = N_1(\xi_2) I_{s\max} + N_2(\xi_2) I_{s\min}$$

where $\xi_2 = 1/I_z$, $I_{s\max} = 1/I_{z\min}$, $I_{s\min} = 1/I_{z\max}$, and $N_1(\xi_1)$ and $N_2(\xi_2)$ are defined similar to (5).

By defining $h_i(\xi) = M_k(\xi_1)N_j(\xi_2)$, where $i = 1 \sim 4$, $k = 1, 2$, $j = 1, 2$, it obtains $h_i(\xi) \geqslant 0$ and $\sum_{i=1}^4 h_i(\xi) = 1$, and the system in (4) with varying vehicle mass and moment of inertia can be expressed in polytopic form as

$$\dot{x}(t) = \sum_{i=1}^4 h_i(\xi)\left[A_i x(t) + B_{1i} w(t) + B_{2i} u(t)\right] \tag{6}$$

where matrices A_i, B_{1i}, and B_{2i}, $i = 1, 2, 3, 4$ are obtained by replacing $1/m$ and $1/I_z$ in matrices A, B_1, and B_2, with $m_{s\max}$ and $m_{s\min}$ and $I_{s\max}$ and $I_{s\min}$, respectively.

When the lateral acceleration is high, the tire forces are no longer linearly proportional to the slip angles due to the tire saturation property. That is, the cornering stiffness used in the linear tire model should be varied when the road friction changes or when the nonlinear tire domain is reached. Taking cornering stiffness variations into account, the linear tire model could correct the cornering stiffness via the uncertain variables $\Delta C_{\alpha f}$ and $\Delta C_{\alpha r}$ as [14]

$$\begin{aligned} F_{yf}(t) &= (C_{\alpha f} + \Delta C_{\alpha f})\alpha_f(t) \\ F_{yr}(t) &= (C_{\alpha r} + \Delta C_{\alpha r})\alpha_r(t). \end{aligned} \tag{7}$$

If the slip angle is controlled to be small enough so that it is always located in the linear region, then using (7) could reflect most of the road friction conditions. Considering the cornering stiffness uncertainties in the model, we get

$$\begin{aligned} \dot{x}(t) &= \sum_{i=1}^4 h_i(\xi)[(A_i+\Delta A_i)x(t)+(B_i+\Delta B_i)w(t)+B_{2i}u(t)] \\ &= (A_h+\Delta A_h)x(t)+(B_{1h}+\Delta B_{1h})w(t)+B_{2h}u(t) \end{aligned} \tag{8}$$

where $A_h = \sum_{i=1}^4 h_i(\xi)A_i$, $B_{1h} = \sum_{i=1}^4 h_i(\xi)B_{1i}$, and $B_{2h} = \sum_{i=1}^4 h_i(\xi)B_{2i}$. $\Delta A_h = \sum_{i=1}^4 h_i(\xi)\Delta A_i$, and ΔA_i represents the uncertainty caused by the uncertain variables $\Delta C_{\alpha f}$ and $\Delta C_{\alpha r}$ on matrix A_i. When a norm-bounded approach is used, ΔA_i can be expressed as $\Delta A_i = HFE_i$, where H and E_i are known constant matrices with appropriate dimensions, and F is an unknown matrix function bounded by $F^T F \leqslant I$. Hence, $\Delta A_h = \sum_{i=1}^4 h_i(\xi)HFE_i = HFE_h$, where $E_h = \sum_{i=1}^4 h_i(\xi)E_i$. Similarly, $\Delta B_{1h} = \sum_{i=1}^4 h_i(\xi)\Delta B_{1i}$, and ΔB_{1i} represents the uncertainty caused by the uncertain variables $\Delta C_{\alpha f}$ and $\Delta C_{\alpha r}$ on matrix B_{1i}, and $\Delta B_{1i} = H_1 F_1 E_{1i}$, where H_1 and E_{1i} are known constant matrices with appropriate dimensions, and F_1 is an unknown matrix function bounded by $F_1^T F_1 \leqslant I$. Accordingly, $\Delta B_{1h} = \sum_{i=1}^4 h_i(\xi)H_1 F_1 E_{1i} = H_1 F_1 E_{1h}$, where $E_{1h} = \sum_{i=1}^4 h_i(\xi)E_{1i}$.

Furthermore, the yaw moment should be bounded in a real application due to some physical constraints resulting from both the actuation system and the tire–road conditions. Taking $\bar{u}(t)$ as the bounded yaw moment, the system in (8) is expressed as

$$\begin{aligned} \dot{x}(t) &= (A_h + \Delta A_h)x(t) + (B_{1h} + \Delta B_{1h})w(t) + B_{2h}\bar{u}(t) \\ &= (A_h + \Delta A_h)x(t) + (B_{1h} + \Delta B_{1h})w(t) \\ &\quad + B_{2h}\frac{1+\varepsilon}{2}u(t) + B_{2h}\left(\bar{u}(t) - \frac{1+\varepsilon}{2}u(t)\right) \end{aligned} \tag{9}$$

where $\bar{u}(t) = \mathrm{sat}(u(t))$, $\mathrm{sat}(u(t))$ is a saturation function of control input $u(t)$, and $0 < \varepsilon < 1$.

III. Robust Controller Design

The yaw-moment controller is constructed as

$$u(t) = Kx(t) \tag{10}$$

where K is the state feedback gain matrix to be designed. To realize good handling and stability, the sideslip angle and the yaw rate are defined as two control outputs, i.e.,

$$\begin{aligned} z_1(t) &= \beta(t) = [1 \quad 0]x(t) = C_1x(t) \\ z_2(t) &= r(t) = [0 \quad 1]x(t) = C_2x(t). \end{aligned} \tag{11}$$

Generally, the desired sideslip angle is given as zero, and the desired yaw rate is defined in terms of vehicle speed and steering input angle as [15]

$$r_d(t) = \frac{v}{l(1+k_{us}v^2)}\delta(t) \tag{12}$$

where $l = l_f + l_r$, and k_{us} is a stability factor. To make a good compromise between sideslip angle and yaw rate, the control objective is defined as minimizing the sideslip angle $\beta(t)(z_1(t))$ subject to the yaw rate $r(t)$ $(z_2(t))$ being smaller than a given number. To make the controller adequately performing for a wide range of maneuvers, the L_2 gain is chosen as the performance measure for $z_1(t)$, which is defined as

$$\|T_{z_1w}\|_\infty = \sup_{\|w(t)\|_2 \neq 0} \frac{\|z_1(t)\|_2}{\|w(t)\|_2} \tag{13}$$

where $\|z_1(t)\|_2^2 = \int_0^\infty z_1^T(t)z_1(t)dt,\ \|w(t)\|_2^2 = \int_0^\infty w^T(t)w(t)dt$, and the performance measure

$$\|z_2(t)\|_\infty < \gamma \|w(t)\|_2 \tag{14}$$

is required for $z_2(t)$, where $\gamma > 0$ is a given smaller number, and $\|z_2(t)\|_\infty = \sup_{t\in[0,\infty)} \sqrt{z_2^T(t)z_2(t)}$.

The controller design is given in the following theorem.

Theorem 1: For the given scalars $\gamma > 0$, $\rho > 0$, $1 > \varepsilon > 0$, and $u_{\lim} > 0$, where $u_{\lim}$ is control input limit, and matrices H, H_1, E_i, and E_{1i}, $i = 1, 2, 3, 4$, the system in (9) with the controller in (10) is quadratically stable, and the L_2 gain $\|T_{z_1w}\|_\infty$ defined by (13) is less than γ, and $\|z_2(t)\|_\infty < \gamma\|w(t)\|_2$ if there exist matrices $Q > 0$ and Y and scalars $\epsilon_1 > 0$, $\epsilon_2 > 0$, and $\epsilon_3 > 0$ satisfying the LMIs

$$\begin{bmatrix} \Xi_{11} & \Xi_{12} \\ * & \Xi_{22} \end{bmatrix} < 0 \tag{15}$$

$$\begin{bmatrix} \left(\frac{u_{\lim}}{\varepsilon}\right)^2 I & Y \\ Y^T & Q\rho^{-1} \end{bmatrix} \geqslant 0 \tag{16}$$

$$\begin{bmatrix} Q & QC_2^T \\ C_2Q & I \end{bmatrix} > 0 \tag{17}$$

where

$$\Xi_{11} = \begin{bmatrix} \Lambda & Y^T & QC_1^T \\ * & -\epsilon_1^{-1}\left(\frac{2}{1-\varepsilon}\right)^2 I & 0 \\ * & * & -I \end{bmatrix}$$

with $\Lambda = QA_i^T + A_iQ + (1+\varepsilon/2)[Y^TB_{2i}^T + B_{2i}Y] + \epsilon_1^{-1}B_{2i}B_{2i}^T + \epsilon_2^{-1}HH^T + \epsilon_3^{-1}H_1H_1^T$

$$\Xi_{12} = \begin{bmatrix} B_{1i} & 0 & QE_i^T \\ 0 & 0 & 0 \\ 0 & 0 & 0 \end{bmatrix}$$

$$\Xi_{22} = \begin{bmatrix} -\gamma^2 I & E_{1i}^T & 0 \\ * & -\epsilon_3^{-1}I & 0 \\ * & * & -\epsilon_2^{-1}I \end{bmatrix}$$

where $i = 1, 2, 3, 4$. Moreover, the controller gain can be obtained as $K = YQ^{-1}$.

Proof: Let us define a Lyapunov function for the system in (9) as

$$V(x(t)) = x^T(t)Px(t) \tag{18}$$

where P is a positive definite matrix.

By differentiating (18), we obtain

$$\dot{V}(x(t)) = \dot{x}^T(t)Px(t) + x^T(t)P\dot{x}(t). \tag{19}$$

By using [16] and a norm-bounded approach presented in [17], together with (9) and (10), we have

$$\begin{aligned} \dot{V}(x(t)) \leqslant\ & x^T(t)\Theta x(t) + w^T(t)B_{1h}^TPx(t) + x^T(t)PB_{1h}w(t) \\ & + \epsilon_3 w^T(t)E_{1h}^TE_{1h}w(t) + \epsilon_3^{-1}x^T(t)PH_1H_1^TPx(t) \end{aligned} \tag{20}$$

where $\Theta = A_h^TP + PA_h + (B_{2h}(1+\varepsilon/2)K)^TP + PB_{2h}(1+\varepsilon/2)K + \epsilon_1(1-\varepsilon/2)^2K^TK + \epsilon_1^{-1}PB_{2h}B_{2h}^TP + \epsilon_2E_h^TE_h + \epsilon_2^{-1}PHH^TP$.

Adding $z_1^T(t)z_1(t) - \gamma^2w^T(t)w(t)$, $\gamma > 0$ to two sides of (20) yields

$$\dot{V}(x(t)) + z_1^T(t)z_1(t) - \gamma^2w^T(t)w(t) \leqslant \begin{bmatrix} x(t) \\ w(t) \end{bmatrix}^T \Pi \begin{bmatrix} x(t) \\ w(t) \end{bmatrix} \tag{21}$$

where Π is defined as

$$\Pi = \begin{bmatrix} \Pi_{11} & PB_{1h} \\ B_{1h}^TP & -\gamma^2I + \epsilon_3E_{1h}^TE_{1h} \end{bmatrix} \tag{22}$$

with $\Pi_{11} = A_h^TP + PA_h + C_{1h}^TC_{1h} + \epsilon_2E_h^TE_h + (B_{2h}(1+\varepsilon/2)K)^TP + PB_{2h}(1+\varepsilon/2)K + \epsilon_1(1-\varepsilon/2)^2K^TK + \epsilon_1^{-1}PB_{2h}B_{2h}^TP + \epsilon_2^{-1}PHH^TP + \epsilon_3^{-1}PH_1H_1^TP$.

Let us consider $\Pi < 0$. Then, $\dot{V}(x(t)) + z_1^T(t)z_1(t) - \gamma^2w^T(t)w(t) \leqslant 0$, and the L_2 gain defined in (13) is less than γ with the initial condition $x(0) = 0$. When the disturbance is zero, i.e., $w(t) = 0$, it can be inferred from (21) that if $\Pi < 0$, then $\dot{V}(x(t)) < 0$, and the system in (9) with the controller in (10) is quadratically stable.

Premultiplying and postmultiplying (22) by $\mathrm{diag}(P^{-1} \quad I)$ and its transpose, respectively, and defining $Q = P^{-1}$, $Y = KP^{-1}$, the condition $\Pi < 0$ is equivalent to

$$\Xi = \begin{bmatrix} \Xi_{11} & B_1 \\ B_1^T & -\gamma^2I + \epsilon_3E_{1h}^TE_{1h} \end{bmatrix} < 0 \tag{23}$$

where $\Xi_{11} = QA_h^T + A_hQ + (1+\varepsilon/2)Y^TB_{2h}^T + (1+\varepsilon/2)B_{2h}Y + \epsilon_1(1-\varepsilon/2)^2Y^TY + \epsilon_1^{-1}B_{2h}B_{2h}^T + QC_{1h}^TC_{1h}Q + \epsilon_2QE_h^TE_hQ + \epsilon_2^{-1}HH^T + \epsilon_3^{-1}H_1H_1^T$. By the Schur complement, the definitions $A_h = \sum_{i=1}^4 h_i(\xi)A_i$, $B_{1h} = \sum_{i=1}^4 h_i(\xi)B_{1i}$, $B_{2h} = \sum_{i=1}^4 h_i(\xi)B_{2i}$, $E_h = \sum_{i=1}^4 h_i(\xi)E_i$, and $E_{1h} = \sum_{i=1}^4 h_i(\xi)E_{1i}$, and the facts $h_i(\xi) \geqslant 0$ and $\sum_{i=1}^4 h_i(\xi) = 1$, $\Xi < 0$ is equivalent to (15).

TABLE I
PARAMETER VALUES OF THE CASE STUDY VEHICLE

Symbol	Meaning	Value
m	vehicle total mass	1298.9 kg
I_z	vehicle moment of inertia about yaw axis	1627 kg·m^2
k_{us}	stability factor	0.03
l_f	distance of CG from front axle	1 m
l_r	distance of CG from rear axle	1.454 m

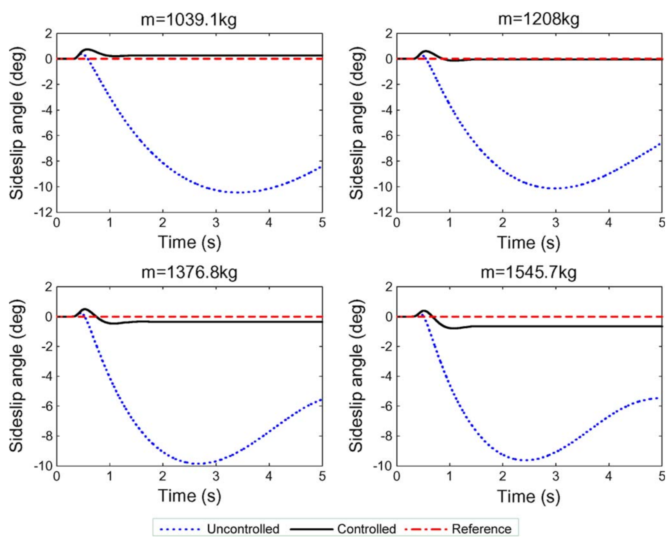

Fig. 2. Sideslip angle responses under J-turn maneuver with different vehicle masses.

By referring to [18] and [19], respectively, conditions (16) and (17) can be obtained without much difficulty, whose proofs are omitted here for brevity.

To make the sideslip angle as small as possible, the following optimization problem is applied:

$$\min \gamma \text{ subject to LMIs } (15)-(17). \tag{24}$$

This is a convex optimization problem that can efficiently be solved by means of Matlab LMI Toolbox software.

IV. SIMULATION RESULTS

In this section, a yaw-plane 2DOF vehicle dynamics model with nonlinear Dugoff tire model is used to validate the effectiveness of the proposed controller. The parameters used for the vehicle model are listed in Table I. The robust controller is designed using the previously proposed approach, where 20% variations on vehicle mass and moment of inertia are considered, respectively, and 50% variation on cornering stiffness is assumed. A J-turn maneuver, which is produced from the ramp steering input (the maximum degree is 6°), is used to testify the vehicle lateral dynamics performance. In the following simulations, if it is not mentioned, then the nominal values for m and I_z are as given in Table I, the saturation limit $u_{\lim} = 3000$ Nm, and the road friction coefficient $\mu = 0.9$ will be used.

We first check the vehicle lateral dynamic performance in terms of the change of vehicle mass. Both vehicle dynamics with and without controller are checked to show the effects of the proposed controller. Figs. 2 and 3 show the simulation results of sideslip angle and yaw rate under J-turn maneuver with four different vehicle masses. From Figs. 2 and 3, we observe that the sideslip angle and yaw rate responses of the controlled system are all better than the uncontrolled system, regardless of the change of vehicle mass. In particular, the sideslip angles are all close to the reference value, i.e., zero degree (i.e., desired sideslip angle), and the yaw rates are all smaller than the corresponding uncontrolled system responses.

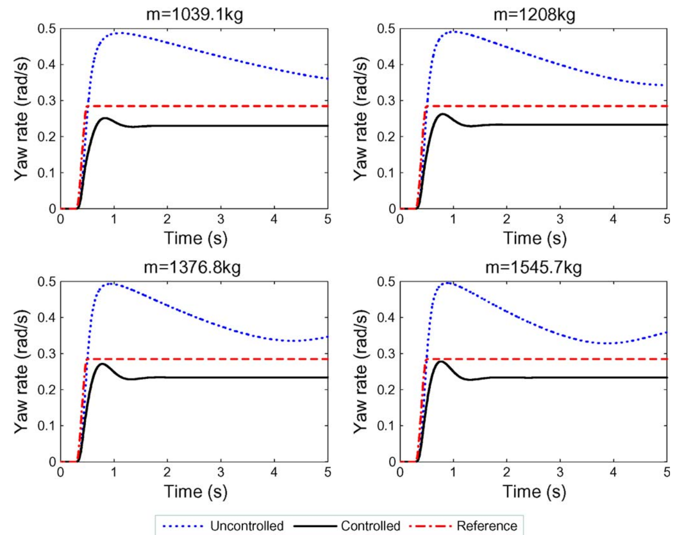

Fig. 3. Yaw-rate responses under J-turn maneuver with different vehicle masses.

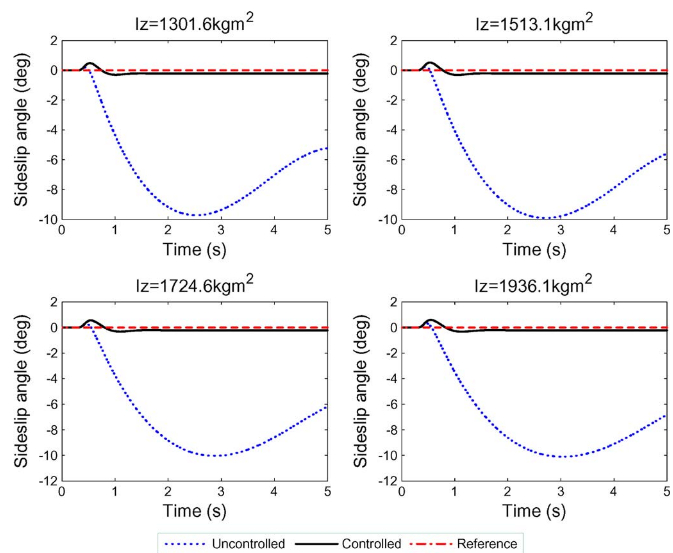

Fig. 4. Sideslip angle responses under J-turn maneuver with different moments of inertia.

We now check the vehicle lateral dynamic performance in terms of the change of moment of inertia. Fig. 4 shows the simulation result of sideslip angle under J-turn maneuver with four different moments of inertia. The simulation result of yaw rate is omitted here to save space. We can observe from Fig. 4 that the sideslip angle responses of the controlled system are all better than the uncontrolled system, regardless of the change of moment of inertia.

The robustness of the controller to the cornering stiffness uncertainties is checked by changing the road surface. Fig. 5 shows the response of sideslip angle under J-turn maneuver with four different road frictions. It is observed from Fig. 5 that the sideslip angle responses of

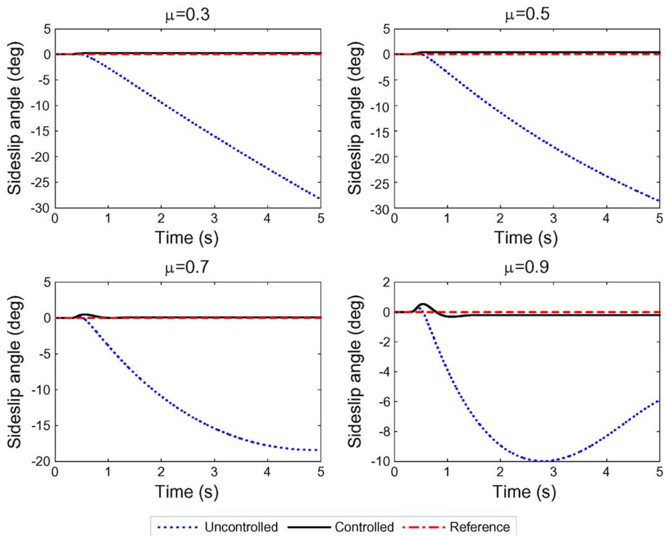

Fig. 5. Sideslip angle responses under J-turn maneuver with different road surfaces.

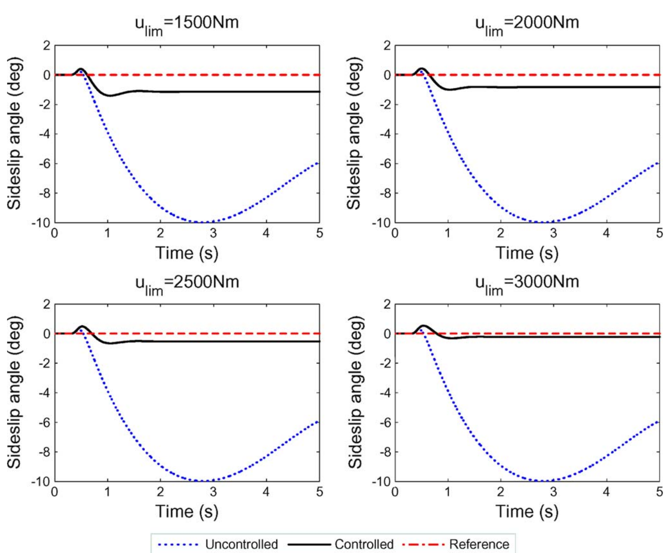

Fig. 6. Sideslip angle responses under J-turn maneuver with different saturation limitations.

the controlled system are all close to the reference value, even with the variation on road friction. On the contrary, the sideslip angle responses of the uncontrolled system largely vary. Since the sideslip angle can be controlled in a very small range, the corrected linear tire model could cover most of the road conditions, and the robust controller can make the vehicle lateral dynamics insensitive to the variation in road conditions.

Similarly, the actuator saturation limit is varied to check the controller's performance with different capacities. For every actuator-saturation limit, the controller will be redesigned. The sideslip angle responses are plotted in Fig. 6, respectively, for saturation limit changing from 1500 to 3000 Nm. It can be seen from this figure that the sideslip angles of the controlled systems are all close to their references. However, different saturation limits will make the controller show different performances. A high saturation limit enables a large yaw moment being applied to the vehicle so that the vehicle-handling performance is improved.

V. Summary

A robust yaw-moment controller has been designed in this paper. The parameter uncertainties on vehicle mass, moment of inertia, cornering stiffness, and control saturation are considered in the controller design process, which makes the controller more robust and the implementation more practical. The control objective is to stabilize the closed-loop system with optimal performance on sideslip angle and yaw rate subject to parameter uncertainties and control saturation. By derivation, the controller design is formalized as a convex optimization problem with solving LMIs. Simulation results are used to validate the performance of the designed controller.

References

[1] J. He, D. A. Crolla, M. C. Levesley, and W. J. Manning, "Coordination of active steering, driveline, and braking for integrated vehicle dynamics control," *Proc. Inst. Mech. Eng. D, J. Automobile Eng.*, vol. 220, no. 10, pp. 1401–1420, 2006.

[2] F. Yu, D. F. Li, and D. A. Crolla, "Integrated vehicle dynamics control-state-of-the art review," in *Proc. IEEE Vehicle Power Propuls. Conf.*, Harbin, China, 2008, pp. 1–6.

[3] A. Mirzaei, M. Moallem, B. M. Dehkordi, and B. Fahimi, "Design of an optimal fuzzy controller for antilock braking systems," *IEEE Trans. Veh. Technol.*, vol. 55, no. 6, pp. 1725–1730, Nov. 2006.

[4] T. Shim, S. Chang, and S. Lee, "Investigation of sliding-surface design on the performance of sliding mode controller in antilock braking systems," *IEEE Trans. Veh. Technol.*, vol. 57, no. 2, pp. 747–759, Mar. 2008.

[5] S. Mammar and D. Koenig, "Vehicle handling improvement by active steering," *Vehicle Syst. Dyn.*, vol. 38, no. 3, pp. 211–242, Sep. 2002.

[6] S. C. Baslamisli, I. E. Kose, and G. Anlas, "Gain-scheduled integrated active steering and differential control for vehicle handling improvement," *Vehicle Syst. Dyn.*, vol. 47, no. 1, pp. 99–119, Jan. 2009.

[7] M. Abe, "Vehicle dynamics and control for improving handling and active safety: From four-wheel steering to direct yaw moment control," in *Proc. Inst. Mech. Eng. K, J. Multi-Body Dyn.*, 1999, vol. 213, no. 2, pp. 87–101.

[8] E. Esmailzadeh, G. R. Goodarzi, and G. R. Vossoughi, "Optimal yaw moment control law for improved vehicle handling," *Mechatronics*, vol. 13, no. 7, pp. 659–675, Sep. 2003.

[9] B. L. Boada, M. J. L. Boada, and V. Diaz, "Fuzzy-logic applied to yaw moment control for vehicle stability," *Vehicle Syst. Dyn.*, vol. 43, no. 10, pp. 753–770, Oct. 2005.

[10] M. Canale, L. Fagiano, M. Milanese, and P. Borodani, "Robust vehicle yaw control using an active differential and IMC techniques," *Control Eng. Pract.*, vol. 15, no. 8, pp. 923–941, Aug. 2007.

[11] S. Antonov, A. Fehn, and A. Kugi, "A new flatness-based control of lateral vehicle dynamics," *Vehicle Syst. Dyn.*, vol. 46, no. 9, pp. 789–801, Sep. 2008.

[12] W. J. Manning and D. A. Crolla, "A review of yaw rate and sideslip controllers for passenger vehicles," *Trans. Inst. Meas. Control*, vol. 29, no. 2, pp. 117–135, 2007.

[13] G. Yin, N. Chen, and P. Li, "Improving handling stability performance of fourwheel steering vehicle via μ-synthesis robust control," *IEEE Trans. Veh. Technol.*, vol. 56, no. 5, pp. 2432–2439, Sep. 2007.

[14] G. Baffet, A. Charara, D. Lechner, and D. Thomas, "Experimental evaluation of observers for tire-road forces, sideslip angle and wheel cornering stiffness," *Vehicle Syst. Dyn.*, vol. 46, no. 6, pp. 501–520, Jun. 2008.

[15] S. Zheng, H. Tang, Z. Han, and Y. Zhang, "Controller design for vehicle stability enhancement," *Control Eng. Pract.*, vol. 14, no. 12, pp. 1413–1421, Dec. 2006.

[16] H. Du, J. Lam, and K. Y. Sze, " H_∞ disturbance attenuation for uncertain mechanical systems with input delay," *Trans. Inst. Meas. Control*, vol. 27, no. 1, pp. 37–52, 2005.

[17] J. H. Kim and F. Jabbari, "Actuator saturation and control design for buildings under seismic excitation," *J. Eng. Mech.*, vol. 128, no. 4, pp. 403–412, Apr. 2002.

[18] Y.-Y. Cao and Z. Lin, "Robust stability analysis and fuzzy-scheduling control for nonlinear systems subject to actuator saturation," *IEEE Trans. Fuzzy Syst.*, vol. 11, no. 1, pp. 57–67, Feb. 2003.

[19] H. Du and J. Lam, "Energy-to-peak performance controller design for building via static output feedback under consideration of actuator saturation," *Comput. Struct.*, vol. 84, no. 31/32, pp. 2277–2290, Dec. 2006.